PHYSICS

Experimentally reducing the quantum measurement back action in work distributions by a collective measurement

Kang-Da Wu[1,2], Yuan Yuan[1,2], Guo-Yong Xiang[1,2]*, Chuan-Feng Li[1,2], Guang-Can Guo[1,2], Martí Perarnau-Llobet[3,4]*

In quantum thermodynamics, the standard approach to estimating work fluctuations in unitary processes is based on two projective measurements, one performed at the beginning of the process and one at the end. The first measurement destroys any initial coherence in the energy basis, thus preventing later interference effects. To decrease this back action, a scheme based on collective measurements has been proposed by Perarnau-Llobet *et al*. Here, we report its experimental implementation in an optical system. The experiment consists of a deterministic collective measurement on two identically prepared qubit states, encoded in the polarization and path degree of a single photon. The standard two-projective measurement approach is also experimentally realized for comparison. Our results show the potential of collective schemes to decrease the back action of projective measurements, and capture subtle effects arising from quantum coherence.

INTRODUCTION

Quantum coherence lies at the heart of quantum physics. Yet, its presence is subtle to observe, as projective measurements inevitably destroy it. In the context of quantum thermodynamics, this tension becomes apparent in work fluctuations: Whereas projective energy measurements are commonly used to measure them (*1*, *2*), they also lead to work distributions that are independent of the initial coherence in the energy basis. This limitation has motivated alternative proposals for defining and measuring work in purely coherent evolutions (*3*–*18*), which include Gaussian (*5*–*8*), weak (*14*–*16*), and collective measurements (CMs) (*17*). These different theoretical proposals aim at reducing the back action induced by projective measurements, thus allowing the preservation of some coherent interference effects. This quest is particularly relevant as, when the system is left unobserved, quantum coherence can play an important role in several thermodynamic tasks, e.g., in work extraction (*19*, *20*) and heat engines (*21*–*24*). Quantum coherence can be seen as a source of free energy, which is destroyed by projective energy measurements (*25*, *26*).

Here, we report the experimental investigation of reducing quantum measurement back action in work distribution using CMs on two identically prepared qubit states. We implement the proposal of (*17*) in an all-optical setup, which can be used to efficiently simulate quantum coherent processes. The standard two-projective energy measurement (TPM) scheme (*1*, *2*) to measure work is also experimentally simulated for comparison. The experimental results show the capability of CM to capture coherent effects and reduce the measurement back action, which is quantified as the fidelity between the probability distributions of the final measured and unmeasured states.

Moreover, the potential application of these results goes beyond quantum thermodynamics, as deterministic CMs play a key role in quantum information, being relevant for numerous tasks such as quantum metrology (*27*, *28*), tomography (*29*, *30*), and state manipulation (*31*).

[1]CAS Key Laboratory of Quantum Information, University of Science and Technology of China, Hefei 230026, People's Republic of China. [2]CAS Center for Excellence in Quantum Information and Quantum Physics, University of Science and Technology of China, Hefei 230026, People's Republic of China. [3]Max-Planck-Institut für Quantenoptik, Hans-Kopfermann-Str. 1, D-85748 Garching, Germany. [4]Munich Center for Quantum Science and Technology (MCQST), Schellingstr. 4, D-80799 München, Germany.
*Corresponding author. Email: gyxiang@ustc.edu.cn (G.-Y.X.); marti.perarnau@mpq.mpg.de (M.P.-L.)

RESULTS

Theoretical framework

The scenario considered here consists of a quantum state ρ and a Hamiltonian H. The system is taken to be thermally isolated, and it can only be modified by externally driving H. We consider processes in which H is transformed up to H', and as a consequence, the state evolves under a unitary evolution U, $\rho \rightarrow U\rho U^\dagger$. The average energy for this process is given by

$$\langle W \rangle = \mathrm{Tr}(H\rho) - \mathrm{Tr}(H' U\rho U^\dagger) \quad (1)$$

where the energy difference can be identified with unmeasured average work. However, when one attempts to measure it, the average measured work usually differs from Eq. 1 due to measurement back action (*1*, *3*, *6*, *17*, *32*).

In the standard approach to measuring work in quantum systems (*1*, *2*), one implements two energy measurements, of H and H', before and after the evolution U. More precisely, expanding the Hamiltonians in the bra-ket representation, as $H = \sum_i E_i |i\rangle\langle i|$ and $H' = \sum_{j'} E_{j'}' |j'\rangle\langle j'|$, the TPM consists of the following:

1) Projective measurement of H on ρ, yielding outcome E_i with probability $\rho_{ii} = \langle i|\rho|i\rangle$

2) A unitary evolution U of the postmeasured state, $|i\rangle \rightarrow U|i\rangle$

3) A projective measurement of H' on the evolved state, yielding E_j' with probability $p_{i,j'} = |\langle j'|U|i\rangle|^2$

The TPM work statistics are then given by the random variable $w^{(ij')} = E_i - E_{j'}'$ with a corresponding probability $P_{\mathrm{TPM}}^{(ij')} = \rho_{ii} p_{i,j'}$ assigned to the transition $|i\rangle \rightarrow |j'\rangle$. The average measured work, $\langle W_{\mathrm{TPM}} \rangle \equiv \sum_{ij} P_{\mathrm{TPM}}^{(ij')} w^{(ij')}$, can be written as

$$\langle W_{\mathrm{TPM}} \rangle = \mathrm{Tr}(H\mathcal{D}_H[\rho]) - \mathrm{Tr}(H' U\mathcal{D}_H[\rho]U^\dagger) \quad (2)$$

where $\mathcal{D}_H[\rho]$ is the dephasing operator, removing all the coherence of ρ, which yields a classical mixture of energy states of H. Hence, $\langle W_{\mathrm{TPM}} \rangle$ differs from the unmeasured average work in Eq. 1 when ρ is coherent (and $[H, U^\dagger H' U] \neq 0$). Furthermore, the extractable work from $\mathcal{D}_H[\rho]$ is lower than that from ρ, as the latter is generally more pure. This can be seen by noting that the nonequilibrium free energy, which characterizes

the extractable work from a state, decomposes into a contribution arising from $\mathcal{D}_H[\rho]$ and one from the coherent part of ρ (*25*, *26*) [see also appendix A of (*18*)].

To reduce the back action of the TPM scheme, a CM has been proposed (*17*). To describe these measurements, let us now introduce the formalism of generalized measurements, which extends the standard quantum projective measurements. A generalized measurement is defined by a positive operator–valued measure (POVM) (*33*), which is a set of non-negative Hermitian operators $\{M^{(i)}\}$ satisfying the completeness condition $\sum_{\{i\}} M^{(wi)} = \mathbb{I}$. Each operator $M^{(i)}$ is associated to a measurement outcome $w^{(i)}$ of the experiment. Then, given a quantum state ρ, the probability to obtain the $w^{(i)}$ is given by the generalized Born rule

$$P^{(i)} = \mathrm{Tr}(\rho M^{(i)}) \tag{3}$$

Note that the completeness condition ensures that the sum of probability obtained from each outcome i is equal to 1. CMs can then be naturally introduced by taking ρ to be a collection of n independent systems, $\rho = \rho_1 \otimes \rho_2 \otimes \ldots \otimes \rho_n$, so that

$$P^{(i)} = \mathrm{Tr}(\rho_1 \otimes \rho_2 \otimes \ldots \otimes \rho_n M^{(i)}) \tag{4}$$

That is, the measurement acts globally on the n systems. In this work, we consider systems made up of two qubits so that the CMs act globally on a Hilbert space of four dimensions.

At this point, it is useful to express the TPM scheme as a POVM, with elements $M^{(ij')}_{\mathrm{TPM}} = |\langle j'|U|i\rangle|^2 |i\rangle\langle i|$ and probability-assigned $P^{(ij')}_{\mathrm{TPM}} = \mathrm{Tr}(M^{(ij')}_{\mathrm{TPM}}\rho)$, where $|i\rangle\langle i|$ denotes a projection on energy basis i. On the other hand, the CM scheme is defined by a POVM with elements $M^{(ij')}_{\mathrm{CM}}$ that act on two copies of the state, $\rho^{\otimes 2}$, with associated probability $P^{(ij')}_{\mathrm{CM}} = \mathrm{Tr}(M^{(ij')}_{\mathrm{CM}}\rho^{\otimes 2})$. The POVM elements read

$$M^{(ij')}_{\mathrm{CM}} = M^{(ij')}_{\mathrm{TPM}} \otimes \mathbb{I} + \lambda |i\rangle\langle i| \otimes T^{\mathrm{off-diag}}_{j'} \tag{5}$$

where $T^{\mathrm{off-diag}}_{j'}$ is the off-diagonal part of $T_{j'} = U^\dagger |j'\rangle\langle j'|U$ in the $\{|i\rangle\}$ basis. This measurement satisfies two basic properties:

1) When acting upon states with zero coherence, $\rho = \mathcal{D}(\rho)$, the CM scheme reproduces exactly the same statistics of the standard TPM scheme. This is followed by noting that $\mathrm{Tr}(T^{\mathrm{off-diag}}_{j'}\mathcal{D}(\rho)) = 0$ and $\mathrm{Tr}(\mathcal{D}(\rho)) = 1$ in Eq. 5.

2) When acting upon general ρ, the second term of Eq. 5 brings information about the purely coherent part of the evolution. This can be seen by computing the average measured work, $\langle W_{\mathrm{CM}}\rangle = \sum_{i,j'} w^{(ij')} P^{(ij')}_{\mathrm{CM}}$, leading to

$$\langle W_{\mathrm{CM}}\rangle = (1-\lambda)\langle W_{\mathrm{TPM}}\rangle + \lambda\langle W\rangle \tag{6}$$

Hence, the parameter $\lambda \in [0, 1]$ quantifies the degree of measurement back action. In general, λ is given by an optimization procedure, which is described in Materials and Methods, and it can be controlled in our experiment. We also note that other proposals of work measurements in states with quantum coherence, in particular weak or Gaussian measurements, can interpolate between properties 1 and 2 described above. In the limit of strong (weak) measurements, property 1 (2) is satisfied, whereas for intermediate couplings with the apparatus, a tradeoff appears [see (*5*–*8*) for discussions].

With the probabilities $P^{(ij')}$, which can be obtained by either the TPM or CM scheme, the full work distribution is constructed as

$$P(w) = \sum_{ij} P^{(ij')} \delta(w - w^{(ij')}) \tag{7}$$

where δ is a Dirac delta function, which accounts for possible degeneracies in $w^{(ij')}$.

Experimental protocol

We consider the experimental realization of the CM in Eq. 5 on a two-qubit system in a quantum optics setup. The core idea is to encode the first (second) copy into the path (polarization) degree of freedom of a single photon, as illustrated in Fig. 1. Single photons have degenerate Hamiltonians for both polarization and path degree, i.e., $w^{(ij')} = 0$ for all i, j', leading to a priori trivial work distributions $P(w)$ in Eq. 7. Yet, $P(w)$ is a coarse-grained version of the transition probabilities $P^{(ij')}$, and the latter contains all information about the quantum stochastic process. Therefore, we focus on $P^{(ij')}$ and attempt to capture the subtle effect of quantum coherence in the process by working on the experimentally, highly nontrivial two-copy space.

We consider unitary process of the form $U(\theta) = \cos\theta\sigma_z + \sin\theta\sigma_x$, where σ_x and σ_z are Pauli operators and the parameter θ is tunable. For such $U(\theta)$'s, we have $\lambda = \tan\theta$ ($\theta \in [0, \pi/4]$), leading to

$$\begin{aligned} M^{(00')}_{\mathrm{CM}} &= |0\rangle\langle 0| \otimes (\cos^2\theta\mathbb{I} + \sin^2\theta\sigma_x) \\ M^{(01')}_{\mathrm{CM}} &= 2\sin^2\theta|0\rangle\langle 0| \otimes |-\rangle\langle -| \\ M^{(10')}_{\mathrm{CM}} &= 2\sin^2\theta|1\rangle\langle 1| \otimes |+\rangle\langle +| \\ M^{(11')}_{\mathrm{CM}} &= |1\rangle\langle 1| \otimes (\cos^2\theta\mathbb{I} - \sin^2\theta\sigma_x) \end{aligned} \tag{8}$$

with $|\pm\rangle = (|0\rangle \pm |1\rangle)/\sqrt{2}$. These measurement operators $M^{(ij')}_{\mathrm{CM}}$, associated to the transitions $|i\rangle \rightarrow |j'\rangle$, are the ones implemented in the experiment (together with the TPM scheme).

Experimental setup

The whole experimental setup is illustrated in Fig. 1 and can be divided into three modules: state preparation module (A), CM module (B), and TPM module (C). In module A, a single-photon state is generated through a type II beam-like phase-matching β-barium borate crystal pumped by an 80-mW continuous-wave laser (with a central wavelength of 404 nm) via spontaneous parametric down-conversion (*34*). The initial state can be written as $|0\rangle^{\otimes 2}$, with the first (second) state encoding the path (polarization) of the photon. Then, the combined action of BD_1 and $H_{1,2,3}$ transforms the initial state into a two-copy state $|\Phi\rangle^{\otimes 2}$, with

$$|\Phi\rangle = \sqrt{p_0}|0\rangle + \sqrt{p_1}|1\rangle \tag{9}$$

where $p_0(p_1)$ is tunable in our experiments, denoting the population of photons initialized in state $|0\rangle(|1\rangle)$, and $p_0 + p_1 = 1$. Details of this transformation are provided in the Supplementary Materials. Module A also allows the generation of a one-copy qubit state in Eq. 9, which is fed into the TPM measurement.

The CM scheme is deterministically realized in module B of Fig. 1. When $|\Phi\rangle^{\otimes 2}$ enters the CM module, the projector $|i\rangle\langle i|$ ($i = 0, 1$) in Eq. 5 on the first copy (path-encoded) is implemented. The information obtained is then fed into a two-element POVM on the second copy (polarization-encoded). If the outcome of the path measurement

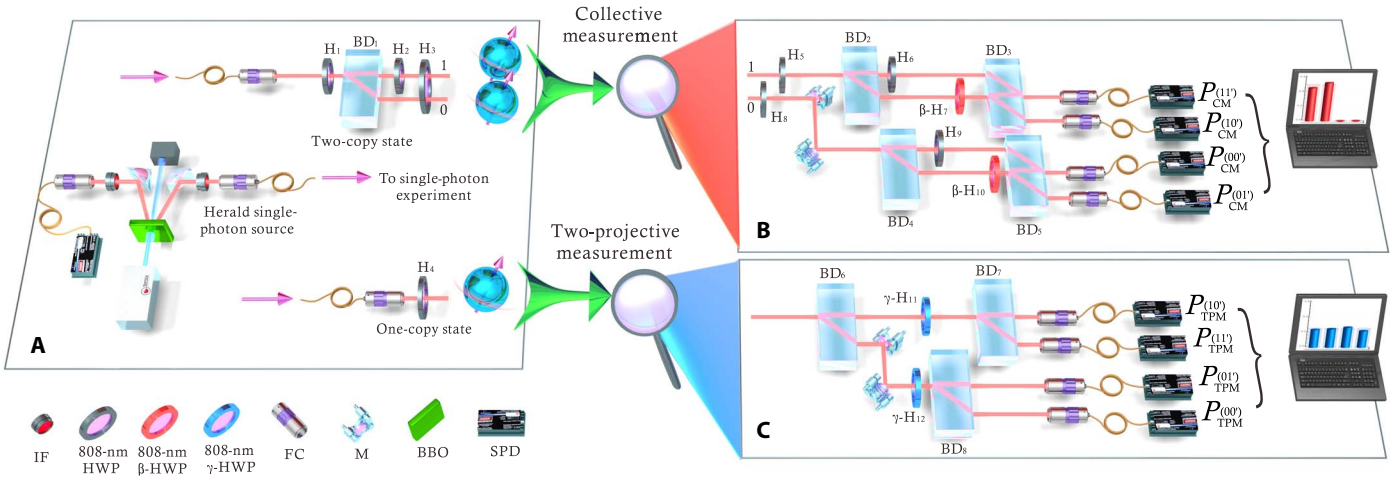

Fig. 1. Experimental setup for both CM and TPM schemes. The setup is divided into three modules: state preparation (**A**), CM (**B**), and TPM (**C**). Module A can generate an arbitrary one-copy polarization-encoded state $|\Phi\rangle$ or a two-copy polarization path–encoded state $|\Phi\rangle^{\otimes 2}$ of a single photon. Module B implements the CM on $|\Phi\rangle^{\otimes 2}$. The rotation angle of two β–half-wave plates (HWPs) is adjustable for different unitary processes $U(\theta)$ with $\cos^2 2\beta = 2\sin^2\theta$. The rotation angles of the other four HWPs are fixed as follows: H_5, 22.5°; H_6, 45°; H_8, 67.5°; H_9, 45°. Module C implements the TPM schemes on $|\Phi\rangle$, and the rotation angle of the two γ-HWPs is adjustable and can implement different $U(\theta)$ with $\theta = 2\gamma$. SPD, single-photon detector; FC, fiber coupler; BD, beam displacer; M, mirror; BBO, β-barium borate; IF, interference filter.

reads 0, then the POVM elements on the second copy are $\cos^2\theta\mathbb{I} + \sin^2\theta\sigma_x$ and $2\sin^2\theta|-\rangle\langle-|$ with outcomes 00′ and 01′; this is done by H_8, H_9, β-H_{10}, BD_4, and BD_5. Note that β-H_{10} implements the unitary transformation $U(\theta)$ through a tunable angle β, satisfying $\cos^2 2\beta = 2\sin^2\theta$. Similarly, if the outcome reads 1, then the POVM elements $2\sin^2\theta|+\rangle\langle+|$ and $\cos^2\theta\mathbb{I} - \sin^2\theta\sigma_x$ are realized through H_5, H_6, β-H_7, BD_2, and BD_3 (see Fig. 1). As in the previous case, β-H_7 implements the unitary $U(\theta)$, with arbitrary θ, by setting θ to $\cos^2 2\beta = 2\sin^2\theta$. See Materials and Methods for more details on module B.

A comparative experiment is performed in module C for simulating the TPM scheme. After the preparation of the one-copy state, the polarization-encoded photon directly enters the TPM measurement, which is conducted by a first polarization measurement, followed by γ-H_{11} and γ-H_{12} implementing the unitary $U(\theta)$ ($\theta = 2\gamma$), and finally sequential projections on the polarization. The parameter γ is tunable and set to $\theta = 2\gamma$ to implement $U(\theta)$. In summary, the four $M_{\mathrm{TPM}}^{(ij')}$ POVM elements can be experimentally realized in this setup, which can simulate coherent processes $U(\theta)$ with arbitrary θ.

Experimental results

We conduct both two schemes for different initial states and unitary processes, with the aim of characterizing the measurement back action. To characterize coherent states and coherent evolutions, we use l-1 norm coherence $C_{l1}(\rho)$ (*35*) and cohering power of a unitary $\mathcal{C}(U)$ (*36*). The l-1 norm coherence measures the degree of interference between different energy bases, and the cohering power quantifies the maximal coherence that can be generated from incoherent states (for more details, see the Supplementary Materials).

The experiments are divided into two parts. In the first part, both measurement schemes are implemented on a pure maximally coherent input state $|+\rangle$ undergoing different unitary processes $U(\theta)$. In the second part, we test the above two measurements on various input $|\Phi\rangle$ while fixing $U(\theta)$.

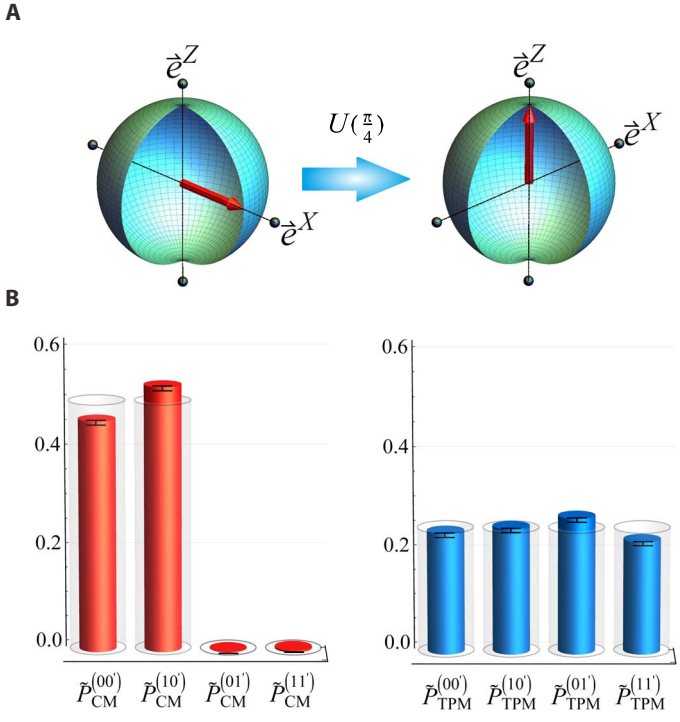

Fig. 2. Transition probabilities for the initial state $|+\rangle$ and the unitary $U(\pi/4)$ from experimental data. Experimental results for the transition probabilities of the CM and TPM measurements correspond to the red and blue cylinders, respectively. (**A**) The factual transition $U(\pi/4)$ takes an initial maximally coherent state $|+\rangle$ to an incoherent pure state $|0\rangle$, and the quantum states are shown by Bloch representation. (**B**) The transition probabilities for the CM are $\tilde{P}_{\mathrm{CM}}^{(00')} = 0.464$, $\tilde{P}_{\mathrm{CM}}^{(10')} = 0.532$, $\tilde{P}_{\mathrm{CM}}^{(10')} = 0.001$, and $\tilde{P}_{\mathrm{CM}}^{(11')} = 0.003$, and the results of the TPM are $\tilde{P}_{\mathrm{TPM}}^{(00')} = 0.244$, $\tilde{P}_{\mathrm{TPM}}^{(10')} = 0.254$, $\tilde{P}_{\mathrm{TPM}}^{(10')} = 0.275$, and $\tilde{P}_{\mathrm{TPM}}^{(11')} = 0.227$. The theoretical fitting values are shown by black-edged transparent cylinders.

To make a quantitative analysis on the back action, we compare the probability distributions of ending in state $|j'\rangle$, with $j' = \{0, 1\}$, for the unmeasured and measured states—by either TPM or CM. The strength of the measurement back action is quantified by the fidelity $\mathcal{F}$ between both distributions so that, for $\mathcal{F} = 1$, there is no back action. The probability distribution of the unmeasured final state can be computed as $P_{\mathrm{Id}}^{(j')} = |\langle j'|U(\theta)|\Phi\rangle|^2$ with $j' = 0, 1$, whereas the measured final distribution is obtained as $\tilde{P}_{\mathrm{CM}}^{(j')} = \Sigma_i \tilde{P}_{\mathrm{CM}}^{(ij')}$ and $\tilde{P}_{\mathrm{TPM}}^{(j')} = \Sigma_i \tilde{P}_{\mathrm{TPM}}^{(ij')}$ for the CM and TPM schemes, respectively, where the superscript in $\tilde{P}$ indicates that it is obtained from experimental data.

To illustrate our results, we first consider the evolution of $|+\rangle \equiv (|0\rangle + |1\rangle)/\sqrt{2}$ toward $|0\rangle$ through $U(\pi/4)$. The measured probabilities $\tilde{P}^{(ij')}$ are shown in Fig. 2, plotted as red and blue cylinders for the CM and TPM schemes, respectively. The theoretical values for both schemes are shown with a black-edged transparent cylinder. We observe strong differences between the TPM and CM distributions, with the latter results naively expected from the unmeasured evolution $|+\rangle \rightarrow |0\rangle$. The probabilities for ending in $0'$ and $1'$ are given by $\tilde{P}_{\mathrm{CM}}^{(0')} = 0.996$ and $\tilde{P}_{\mathrm{CM}}^{(1')} = 0.004$ for the CM and by $\tilde{P}_{\mathrm{TPM}}^{(0')} = 0.498$ and $\tilde{P}_{\mathrm{TPM}}^{(1')} = 0.502$ for the TPM, while the unmeasured evolution yields $P_{\mathrm{Id}}^{(0')} = 1.0$ and $P_{\mathrm{Id}}^{(1')} = 0.0$. The fidelity, which measures the back action, for the above two schemes reads $F_{\mathrm{CM}} = 0.998$ and $F_{\mathrm{TPM}} = 0.706$, respectively.

Experimental results for different coherent processes are shown in Fig. 3. The cohering power is tuned by the rotation angle β of H_7 and H_{10} from 0° to 45°, resulting in a variation from 0 to 1, taking $|+\rangle$ to various ending states (Fig. 3A). The fidelity between the probability distributions of the unmeasured and measured cases, represented by red and blue discs, respectively, is plotted against the cohering power (Fig. 3B). The experimental data agree very well with theoretical predictions, represented by solid lines (details on the calculation of $\mathcal{F}$ are provided in the Supplementary Materials). As the cohering power increases, the TPM scheme becomes more invasive, while the fidelity provided by the CM remains high. The experimentally observed minimal $\mathcal{F}$ via the CM scheme is 0.963, with a cohering power of 0.834, while in the standard TPM approach, the minimal fidelity drops to 0.706. The results show that CM predicts transition probabilities that are closer to the unmeasured evolution.

In the second part of the experiments, the above protocol is tested for a fixed U with a cohering power $\sqrt{3}/2$ on input states with various initialized coherence $C_{l1}(|\Phi\rangle)$ corresponding to different p_0 ranging from 0 to 1 (Fig. 4A). The fidelity for both the CM and TPM schemes is plotted against p_0 in Fig. 4B. In both cases, the experimentally observed minimal fidelity occurs when $p_0 = 0.75$, with 0.906 and 0.799, respectively. The data match those of theoretical fittings very well.

CONCLUSION

Describing work fluctuations in genuinely coherent processes remains a subtle and open question in quantum thermodynamics, although relevant progress has been achieved recently (*3*–*18*, *37*–*39*). Here, we report the first experimental observation of work distributions, or more precisely of transition probabilities, using an implementation based on a CM scheme (*17*). Our experimental results show how the CM scheme can reduce the measurement back action, as compared to the standard TPM scheme, yielding transition probabilities that are closer to the unmeasured evolution. However, a full understanding of the CM approach

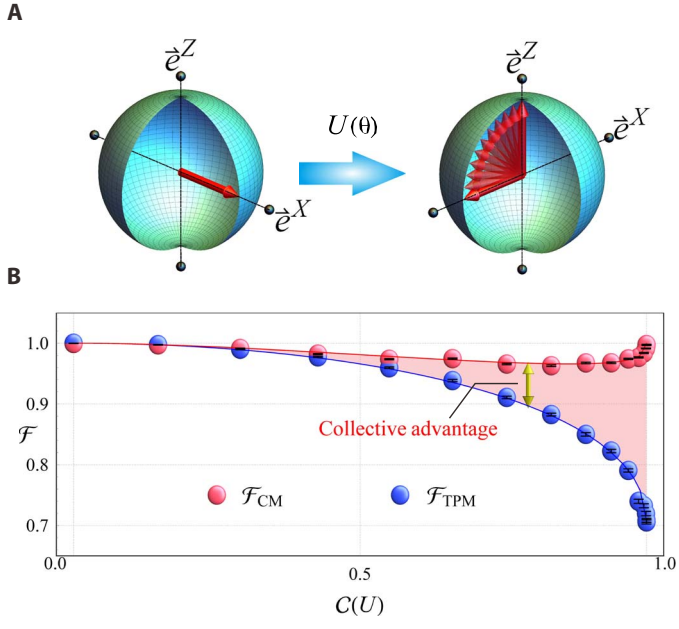

Fig. 3. Measurement back action (obtained from experimental data) for various coherent processes. Experimental results for the measurement back action, quantified by the fidelity between measured and unmeasured final energy distributions, of the TPM (blue) and CM (red) schemes. The results are obtained by fixing the initial state to a maximally coherent state $|+\rangle$ and for various unitary processes $U(\theta)$ with θ between 0° and 45°, mapping a fixed input to a class of pure states, as shown in (**A**). The fidelity in (**B**) is plotted against the cohering power of $U(\theta)$.

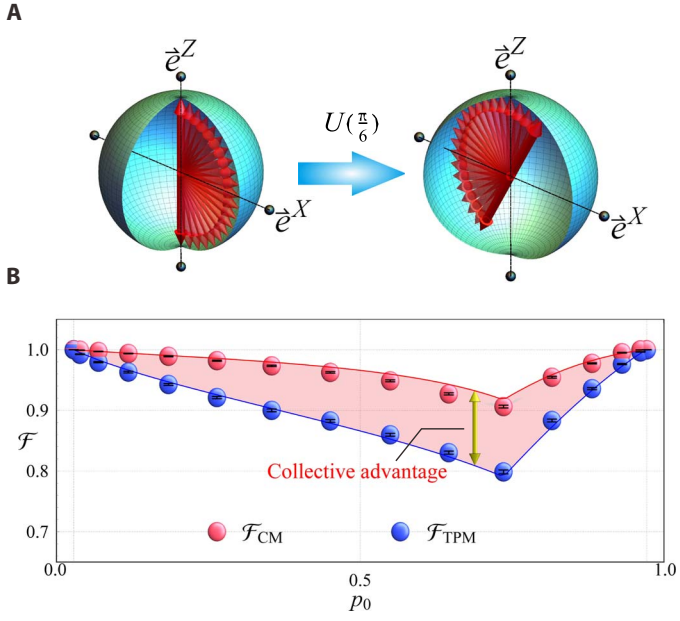

Fig. 4. Measurement back action (obtained from experimental data) for different initial states. Experimental results for the fidelity between the measured and unmeasured final energy distributions, for both the TPM (blue) and CM (red) schemes. The results are obtained for input states of the form $|\Phi\rangle = \sqrt{p_0}|0\rangle + \sqrt{p_1}|1\rangle$ for various values of p_0 between 0 and 1, and $p_0 + p_1 = 1$. The unitary is fixed to $U(\pi/6)$ with a cohering power of $\sqrt{3}/2$, mapping a class of pure states to another class of pure states, as shown in (**A**). The experimental results in (**B**) agree well with theoretical predictions.

is still in progress. For example, while relatively elegant schemes come up in unitary processes, similar constructions for open processes remain a challenging task.

Our experimental results show that quantum coherence can have an effect on the statistics, which complements previous experimental studies of work fluctuations for diagonal states (*40*–*43*). Furthermore, by experimentally demonstrating the strength of the CM scheme for reducing the measurement back action, we hope that our results will stimulate new conceptual and technological developments in quantum thermodynamics and quantum information science, where CMs play an important role in numerous tasks (*28*–*31*).

MATERIALS AND METHODS

Details on the CM scheme

Here, we provided more details on the CM scheme in Eq. 5. Making explicit the dependence on λ

$$M_{\mathrm{CM}}^{(ij')}(\lambda) = M_{\mathrm{TPM}}^{(ij')} \otimes \mathbb{I} + \lambda |i\rangle\langle i| \otimes T_{j'}^{\mathrm{off-diag}} \tag{10}$$

λ is found by the following optimization procedure

$$\lambda = \max_{\alpha} \left(\alpha : M_{\mathrm{CM}}^{(ij')}(\lambda) \geq 0 \; \forall i, j \right) \tag{11}$$

That is, λ is chosen so that the back action is minimized. From Eq. 6, it is clear that, for λ = 1, the back action is minimized and the average measured work by the CM coincides with the unmeasured one in Eq. 1. However, in general, we have the result that $0 < \lambda < 1$, which ensures the positivity of the POVM elements so that this measurement scheme is operationally well defined and can be experimentally implemented.

Details on the experimental CM

In the CM module B, the CM scheme is deterministically realized using six half-wave plates (HWPs) and four beam displacers (BDs), as shown in module B of Fig. 1. In particular, a BD displaces the horizontal (H)–polarized photons about 3 mm away from the original path, while the vertical (V)–polarized photons remain unchanged. The action of an HWP with rotation angle x implements a unitary transformation on polarization-encoded states

$$\begin{aligned} |0\rangle &\rightarrow \cos 2x\,|0\rangle + \sin 2x\,|1\rangle \\ |1\rangle &\rightarrow \sin 2x\,|0\rangle - \cos 2x\,|1\rangle \end{aligned} \tag{12}$$

Note that we have taken $0 \equiv H$ and $1 \equiv V$.

When $|\Phi\rangle^{\otimes 2}$ enters the CM module, the projector $|i\rangle\langle i|$ ($i = 0, 1$) in Eq. 5 on the first copy (path-encoded) is implemented as the photon enters into the 0 or 1 path. Then, the photon goes through a two-element POVM on the second copy (polarization-encoded) according to the measurement outcome of the first copy. If the outcome reads 0 (the path 1), the POVM elements on the second copy are $\cos^2\theta\mathbb{I} + \sin^2\theta\sigma_x$ and $2\sin^2\theta|-\rangle\langle -|$ with outcomes 00′ and 01′.

To realize these POVMs, the rotation angle for H_8 was set to 67.5°, resulting in coherent decomposition of a pure polarization-encoded state in the $|+\rangle$ and $|-\rangle$ basis. In particular, we represented the state of Eq. 9 in the $|\pm\rangle$ basis, i.e., $|\Phi\rangle = \sqrt{p_{0'}}|+\rangle + \sqrt{p_{1'}}|-\rangle$. Then, from Eq. 12, H_8 transforms $|\Phi\rangle$ into $|\Phi'\rangle = \sqrt{p_{0'}}|V\rangle + \sqrt{p_{1'}}|H\rangle$. Note that $|\pm\rangle = \frac{1}{\sqrt{2}}(|0\rangle \pm |1\rangle)$, so $p_0 = \frac{1}{2}(\sqrt{p_{0'}} + \sqrt{p_{1'}})^2$ and $p_1 = \frac{1}{2}(\sqrt{p_{0'}} - \sqrt{p_{1'}})^2$.

Then, after passing BD_4, the H-polarized photon (aforementioned $|-\rangle$ component of $|\Phi\rangle$) is displaced by BD_4 and goes through a β-HWP (H_{10}), with a tunable angle β controlling the parameter θ of the unitary process ($\cos^2 2\beta = 2\sin^2\theta$). β-$HWP_{10}$ transforms the H-polarized photon ($|0\rangle$) into a linearly polarized photon state $\cos 2\beta|0\rangle + \sin 2\beta|1\rangle$. Then, BD_7 displaces the $\cos^2 2\beta$ fraction of the aforementioned $|-\rangle$ component (now H-polarized) for the measurement $M_\theta^{(01)}$. The remaining $\sin^2 2\beta$ part of $|-\rangle$ component (now V-polarized) is combined with the aforementioned $|+\rangle$ component of $|\Phi\rangle$ (now H-polarized) by BD_5 to obtain the measurement $M_\theta^{(00')}$. Similarly, the POVM elements $M_\theta^{(10)}$ and $M_\theta^{(11)}$ can be realized by decomposing the polarization input into $|\pm\rangle$ and letting the $|+\rangle$ component go through an H_7 with angle β. The two β-HWPs are highlighted in red in Fig. 1, as this setup is capable of realizing arbitrary unitary operations $U(\theta)$, where we recall that $\cos^2 2\beta = 2\sin^2\theta$.

SUPPLEMENTARY MATERIALS

Supplementary material for this article is available at http://advances.sciencemag.org/cgi/content/full/5/3/eaav4944/DC1

Section S1. Theoretical aspects

Section S2. Experimental aspects

Table S1. Experimental data for different coherent processes.

Table S2. Experimental data for states with various initial coherence.

REFERENCES AND NOTES

1. M. Campisi, P. Hänggi, P. Talkner, *Colloquium*: Quantum fluctuation relations: Foundations and applications. *Rev. Mod. Phys.* **83**, 771–791 (2011).
2. P. Talkner, E. Lutz, P. Hänggi, Fluctuation theorems: Work is not an observable. *Phys. Rev. E* **75**, 050102 (2007).
3. A. E. Allahverdyan, Nonequilibrium quantum fluctuations of work. *Phys. Rev. E* **90**, 032137 (2014).
4. P. Solinas, S. Gasparinetti, Full distribution of work done on a quantum system for arbitrary initial states. *Phys. Rev. E* **92**, 042150 (2015).
5. G. D. Chiara, A. J. Roncaglia, J. P. Paz, Measuring work and heat in ultracold quantum gases. *New J. Phys.* **17**, 035004 (2015).
6. P. Talkner, P. Hänggi, Aspects of quantum work. *Phys. Rev. E* **93**, 022131 (2016).
7. P. Solinas, S. Gasparinetti, Probing quantum interference effects in the work distribution. *Phys. Rev. A* **94**, 052103 (2016).
8. G. De Chiara, P. Solinas, F. Cerisola, A. J. Roncaglia, Ancilla-assisted measurement of quantum work. arXiv:1805.06047 [quant-ph] (15 May 2018).
9. S. Deffner, J. P. Paz, W. H. Zurek, Quantum work and the thermodynamic cost of quantum measurements. *Phys. Rev. E* **94**, 010103 (2016).
10. H. J. D. Miller, J. Anders, Time-reversal symmetric work distributions for closed quantum dynamics in the histories framework. *New J. Phys.* **19**, 062001 (2017).
11. R. Sampaio, S. Suomela, T. Ala-Nissila, J. Anders, T. G. Philbin, Quantum work in the Bohmian framework. *Phys. Rev. A* **97**, 012131 (2018).
12. B.-M. Xu, J. Zou, L.-S. Guo, X.-M. Kong, Effects of quantum coherence on work statistics. *Phys. Rev. A* **97**, 052122 (2018).
13. P. Solinas, D. V. Averin, J. P. Pekola, Work and its fluctuations in a driven quantum system. *Phys. Rev. B* **87**, 060508 (2013).
14. P. Solinas, H. J. D. Miller, J. Anders, Measurement-dependent corrections to work distributions arising from quantum coherences. *Phys. Rev. A* **96**, 052115 (2017).
15. P. P. Hofer, Quasi-probability distributions for observables in dynamic systems. *Quantum* **1**, 32 (2017).
16. M. Lostaglio, Quantum fluctuation theorems, contextuality, and work quasiprobabilities. *Phys. Rev. Lett.* **120**, 040602 (2018).
17. M. Perarnau-Llobet, E. Bäumer, K. V. Hovhannisyan, M. Huber, A. Acin, No-Go theorem for the characterization of work fluctuations in coherent quantum systems. *Phys. Rev. Lett.* **118**, 070601 (2017).
18. E. Bäumer, M. Lostaglio, M. Perarnau-Llobet, R. Sampaio, Fluctuating work in coherent quantum systems: Proposals and limitations. arXiv:1805.10096 [quant-ph] (25 May 2018).

19. K. Korzekwa, M. Lostaglio, J. Oppenheim, D. Jennings, The extraction of work from quantum coherence. *New J. Phys.* **18**, 023045 (2016).
20. N. Lörch, C. Bruder, N. Brunner, P. P. Hofer, Optimal work extraction from quantum states by photo-assisted Cooper pair tunneling. *Quantum Sci. Technol.* **3**, 035014 (2018).
21. J. Roßnagel, O. Abah, F. Schmidt-Kaler, K. Singer, E. Lutz, Nanoscale heat engine beyond the Carnot limit. *Phys. Rev. Lett.* **112**, 030602 (2014).
22. L. A. Correa, J. P. Palao, D. Alonso, G. Adesso, Quantum-enhanced absorption refrigerators. *Sci. Rep.* **4**, 3949 (2014).
23. M. T. Mitchison, M. P. Woods, J. Prior, M. Huber, Coherence-assisted single-shot cooling by quantum absorption refrigerators. *New J. Phys.* **17**, 115013 (2015).
24. J. Klatzow, J. N. Becker, P. M. Ledingham, C. Weinzetl, K. T. Kaczmarek, D. J. Saunders, J. Nunn, I. A. Walmsley, R. Uzdin, E. Poem, Experimental demonstration of quantum effects in the operation of microscopic heat engines. arXiv:1710.08716 [quant-ph] (24 October 2017).
25. M. Lostaglio, D. Jennings, T. Rudolph, Description of quantum coherence in thermodynamic processes requires constraints beyond free energy. *Nat. Commun.* **6**, 6383 (2015).
26. D. Janzing, Quantum thermodynamics with missing reference frames: Decompositions of free energy into non-increasing components. *J. Stat. Phys.* **125**, 761–776 (2006).
27. V. Giovannetti, S. Lloyd, L. Maccone, Advances in quantum metrology. *Nat. Photonics* **5**, 222–229 (2011).
28. J. G. Bohnet, K. C. Cox, M. A. Norcia, J. M. Weiner, Z. Chen, J. K. Thompson, Reduced spin measurement back-action for a phase sensitivity ten times beyond the standard quantum limit. *Nat. Photonics* **8**, 731–736 (2014).
29. S. Massar, S. Popescu, Optimal extraction of information from finite quantum ensembles. *Phys. Rev. Lett.* **74**, 1259–1263 (1995).
30. Z. Hou, J.-F. Tang, J. Shang, H. Zhu, J. Li, Y. Yuan, K.-D. Wu, G.-Y. Xiang, C.-F. Li, G.-C. Guo, Deterministic realization of collective measurements via photonic quantum walks. *Nat. Commun.* **9**, 1414 (2018).
31. K. C. Cox, G. P. Greve, J. M. Weiner, J. K. Thompson, Deterministic squeezed states with collective measurements and feedback. *Phys. Rev. Lett.* **116**, 093602 (2016).
32. P. Kammerlander, J. Anders, Coherence and measurement in quantum thermodynamics. *Sci. Rep.* **6**, 22174 (2016).
33. M. A. Nielsen, I. Chuang, *Quantum Computation Quantum Information* (Cambridge Univ. Press, 2002).
34. S. Takeuchi, Beamlike twin-photon generation by use of type II parametric downconversion. *Opt. Lett.* **26**, 843–845 (2001).
35. T. Baumgratz, M. Cramer, M. B. Plenio, Quantifying coherence. *Phys. Rev. Lett.* **113**, 140401 (2014).
36. K. Bu, A. Kumar, L. Zhang, J. Wu, Cohering power of quantum operations. *Phys. Lett. A* **381**, 1670–1676 (2017).
37. A. M. Alhambra, L. Masanes, J. Oppenheim, C. Perry, Fluctuating work: From quantum thermodynamical identities to a second law equality. *Phys. Rev. X* **6**, 041017 (2016).
38. J. Åberg, Fully quantum fluctuation theorems. *Phys. Rev. X* **8**, 011019 (2018).
39. H. J. D. Miller, J. Anders, Leggett-Garg inequalities for quantum fluctuating work. *Entropy* **20**, 200 (2018).
40. G. Huber, F. Schmidt-Kaler, S. Deffner, E. Lutz, Employing trapped cold ions to verify the quantum Jarzynski equality. *Phys. Rev. Lett.* **101**, 070403 (2008).
41. T. B. Batalhão, A. M. Souza, L. Mazzola, R. Auccaise, R. S. Sarthour, I. S. Oliveira, J. Goold, G. De Chiara, M. Paternostro, R. M. Serra, Experimental reconstruction of work distribution and study of fluctuation relations in a closed quantum system. *Phys. Rev. Lett.* **113**, 140601 (2014).
42. S. An, J.-N. Zhang, M. Um, D. Lv, Y. Lu, J. Zhang, Z.-Q. Yin, H. T. Quan, K. Kim, Experimental test of the quantum Jarzynski equality with a trapped-ion system. *Nat. Phys.* **11**, 193–199 (2015).
43. F. Cerisola, Y. Margalit, S. Machluf, A. J. Roncaglia, J. P. Paz, R. Folman, Using a quantum work meter to test non-equilibrium fluctuation theorems. *Nat. Commun.* **8**, 1241 (2017).

Acknowledgments

Funding: K.-D.W., Y.Y., G.-Y.X., C.-F.L., and G.-C.G. acknowledge support from the National Nature Science Foundation of China (NSFC; 11574291 and 11774334), National Key R&D Program (2016YFA0301700), and Anhui Initiative in Quantum Information Technologies. M.P.-L. acknowledges support from the Alexander von Humboldt Foundation. and from the Deutsche Forschungsgemeinschaft (DFG,German Research Foundation) under Germany's Excellence Strategy–EXC-2111 – 390814868. **Author contributions:** G.-Y.X. conceived and supervised the project. M.P.-L. designed the theoretical protocol. K.-D.W. designed and implemented the experiments with the assistance from
Y.Y. and G.-Y.X. K.-D.W. analyzed the experimental data with the help of G.-Y.X., C.-F.L., and G.-C.G. K.-D.W., G.-Y.X., and M.P.-L wrote the paper with contributions from all authors. **Competing interests:** The authors declare that they have no competing interests. **Data and materials availability:** All data needed to evaluate the conclusions in the paper are present in the paper and/or the Supplementary Materials. Additional data related to this paper may be requested from the authors.

Submitted 21 September 2018
Accepted 14 January 2019
Published 1 March 2019
10.1126/sciadv.aav4944

Citation: K.-D. Wu, Y. Yuan, G.-Y. Xiang, C.-F. Li, G.-C. Guo, M. Perarnau-Llobet, Experimentally reducing the quantum measurement back action in work distributions by a collective measurement. *Sci. Adv.* **5**, eaav4944 (2019).

ScienceAdvances

Experimentally reducing the quantum measurement back action in work distributions by a collective measurement

Kang-Da Wu, Yuan Yuan, Guo-Yong Xiang, Chuan-Feng Li, Guang-Can Guo and Martí Perarnau-Llobet

Sci Adv **5** (3), eaav4944.
DOI: 10.1126/sciadv.aav4944